Mathematical Biosciences and Engineering

https://www.aimspress.com/journal/mbe

MBE, 23(8): 2259–2286.
DOI: 10.3934/mbe.2026082
Received: 25 March 2026
Revised: 09 May 2026
Accepted: 09 June 2026
Published: 21 July 2026

Research article

Hopf bifurcation and stability in a tumor–immune model with discrete and distributed delays

Rukiye Kara*

Department of Mathematics, Mimar Sinan Fine Arts University, Istanbul, Turkey

* **Correspondence:** Email: rukiye.kara@msgsu.edu.tr; Tel: +90-212-252-0016.

Abstract: We studied a tumor–immune interaction model with one discrete and one distributed delay, where the latter was described by an exponential kernel that captures memory effects in the immune response. We derived the characteristic equation at the interior equilibrium and identified the critical delay and frequency at which a Hopf bifurcation occurs. The direction, stability, and period of the emerging periodic solutions were determined through center manifold and normal form analysis. Numerical simulations confirm the analytical results and show how the kernel parameter modulates the amplitude and frequency of the tumor–immune oscillations. In all tested cases, the coefficients $\mu_2 > 0$ and $\beta_2 < 0$ indicate a stable supercritical Hopf bifurcation, while $T_2 > 0$ shows that the period of the bifurcating periodic solutions increases, consistently with the simulated dynamics.

Keywords: delay differential equations; distributed delay; Hopf bifurcation; center manifold; normal form

1. Introduction

Cancer is still one of the major causes of death and creates a serious burden on patients and healthcare systems. One important reason for tumor growth is how cancer cells interact with the body's immune response [1,2]. The immune response against tumors involves several cell types and signaling mechanisms that contribute to antigen recognition and tumor cell elimination. When tumor antigens are noticed by cells such as macrophages, B cells, or helper T cells, they trigger the activation of cytotoxic T–lymphocytes (CTLs). After they are activated, CTLs can recognize tumor-related antigens and directly attack the tumor cells [3–5].

Mathematical models provide a useful way to examine how tumor cells and immune components interact under different biological assumptions [6–8]. DeLisi and Rescigno [9] proposed a deterministic predator–prey model describing the interaction between solid tumors and killer lymphocytes and analyzed its qualitative behavior. In the same year, Rescigno and DeLisi [10] extended their model

by including two stages of lymphocyte populations, making it more biologically realistic. Kuznetsov et al. [11] developed another model that considered the penetration of effector cells into tumor tissue, validated by experimental data. De Pillis et al. [7], de Pillis and Radunskaya [12], and de Pillis et al. [13] analyzed tumor–immune interactions through mathematical models and evaluated the effects of various treatment strategies using numerical methods.

Liu et al. [14] proposed a two-stage cancer model that explained the dynamic responses of the immune system through Hopf bifurcation and periodic behavior. Pang et al. [15] studied the therapeutic effects of different treatment regimes and analyzed the dynamics of an antitumor model. Pang et al. [16] developed a new model of antitumor immunity based on the principle that lymphocytes mature in two stages and examined its stability and bifurcation properties. Moreover, several mathematical models have been developed to describe the complex interactions between tumor cells and the immune system, often incorporating time delays to capture lags in the immune response and memory effects [3, 5, 17].

In recent years, delay-induced dynamics and Hopf bifurcation phenomena have attracted considerable attention in biological and ecological models. Murugadoss et al. [18] studied a dengue transmission model with two time delays and showed that delays may lead to Hopf bifurcation. Sardar et al. [19] considered a tumor–immune competitive system with multiple delays and analyzed its stability and bifurcation properties. Besides discrete delays, distributed delay terms have also been used to describe memory effects and cumulative past influences in population models. For example, Lou et al. [20] investigated bifurcation phenomena in a diffusive predator–prey system with distributed memory and gestation delay, while Li et al. [21] proposed a two-stage mosquito population model with distributed delay and examined its dynamical behavior. These works suggest that the way past states are incorporated into the model can affect both stability thresholds and oscillatory behavior.

Motivated by these studies, the present work modifies the delayed tumor–immune model of Wang et al. [22], where both the lymphocyte maturation time and the tumor proliferation latency are represented by discrete delays. Here, the lymphocyte maturation delay is kept discrete, since it corresponds to a relatively specific transition from immature to mature lymphocytes. In contrast, the tumor proliferation delay is replaced by an exponentially distributed delay. This is biologically reasonable because tumor proliferation and immune recognition are not instantaneous events; they involve cumulative processes such as antigen release, antigen presentation, and the gradual activation of immune cells. Therefore, the present tumor growth response may depend on a weighted history of past tumor densities rather than on a single past value.

For this mixed discrete–distributed delay model, we derive the characteristic equation at the positive equilibrium, obtain the critical delay for Hopf bifurcation, and verify the transversality condition. We then use center manifold and normal form theory to determine the direction, stability, and period of the bifurcating periodic solutions. Numerical simulations are used to support the analytical results and to illustrate the role of the memory-decay parameter in the resulting tumor–immune oscillations.

2. Model formulation

The model proposed by Wang et al. [22] describes the interactions between immature T–lymphocytes (L_1), mature T–lymphocytes (L_2), and tumor cells (T) as follows:

$$\begin{aligned}
\frac{dL_1}{dt} &= -a\left(L_1 - \frac{b}{a}L_0\right) + \alpha_1 \frac{TL_2}{\eta + T}, \\
\frac{dL_2}{dt} &= aL_1 - \alpha_3 L_2, \\
\frac{dT}{dt} &= cT - \alpha_2 T L_2.
\end{aligned} \tag{2.1}$$

Here, L_0 represents a constant source of immature lymphocytes, and η denotes the saturation parameter in the Michaelis–Menten term. The parameter a is the rate at which immature T–lymphocytes transform into mature T–lymphocytes, while bL_0 denotes the constant production rate of new lymphocytes by the hematopoietic system. The term $\dfrac{\alpha_1 TL_2}{\eta + T}$ corresponds to a Michaelis–Menten-type recruitment mechanism, where α_1 is the maximum recruitment rate. The parameter α_3 represents the inactivation rate of mature T–lymphocytes. The constant c denotes the growth rate of tumor cells, and the term $\alpha_2 TL_2$ models the rate at which mature T–lymphocytes eliminate tumor cells, with α_2 being the corresponding killing coefficient. The delayed tumor–immune interaction model is given as follows:

$$\begin{aligned}
\frac{dL_1}{dt} &= -a\left(L_1 - \frac{b}{a}L_0\right) + \alpha_1 \frac{TL_2}{\eta + T}, \\
\frac{dL_2}{dt} &= aL_1(t - \bar{\tau}_1) - \alpha_3 L_2, \\
\frac{dT}{dt} &= cT(t - \bar{\tau}_2) - \alpha_2 T L_2
\end{aligned} \tag{2.2}$$

where the delay $\bar{\tau}_1$ models the time required for the transition from immature to mature lymphocytes, while $\bar{\tau}_2$ accounts for the latency period in tumor cell proliferation. To simplify the analysis of the delayed tumor model (2.2), the variables and time are nondimensionalized using the following scaling:

$$L_1 - \frac{b}{a}L_0 \;=\; \frac{\alpha_1}{\alpha_2}\, y_1, \qquad L_2 \;=\; \frac{a}{\alpha_2}\, y_2, \qquad T \;=\; \eta\, y_3.$$

The time and delay parameters are scaled via the transformation $t = \frac{1}{a}s$, $\bar{\tau}_1 = \frac{1}{a}\tau_1$, $\bar{\tau}_2 = \frac{1}{a}\tau_2$. Then, the variable s is relabeled as t, and for simplicity of notation, the bars over the delay parameters are dropped, so that τ_1 and τ_2 are used instead. The delayed system (2.2) is reduced to the following dimensionless form:

$$\begin{aligned}
\frac{dy_1}{dt} &= -y_1 + \frac{y_2 y_3}{1 + y_3}, \\
\frac{dy_2}{dt} &= \alpha\, y_1(t - \tau_1) - \beta\, y_2 + \gamma, \\
\frac{dy_3}{dt} &= \delta\, y_3(t - \tau_2) - y_2 y_3.
\end{aligned} \tag{2.3}$$

where $\alpha = \alpha_1/a$, $\beta = \alpha_3/a$, $\gamma = \alpha_2 bL_0/a^2$, and $\delta = c/a$. The second delay in system (2.3) represents the latency in tumor cell proliferation. In the present model, this discrete delay is replaced by a distributed delay, so that the current tumor growth term depends on a weighted contribution of past tumor

densities rather than on one fixed past state. We keep the lymphocyte maturation delay discrete, while the tumor proliferation latency is modeled through a distributed memory term.

By introducing a distributed delay into the tumor equation in place of the second discrete delay, the system is rewritten as

$$\begin{aligned} \frac{dy_1}{dt} &= -y_1 + \frac{y_2 y_3}{1 + y_3}, \\ \frac{dy_2}{dt} &= \alpha y_1(t - \tau_1) - \beta y_2 + \gamma, \\ \frac{dy_3}{dt} &= \delta \int_{-\infty}^{t} F(t - s)\, y_3(s)\, ds - y_2 y_3. \end{aligned} \tag{2.4}$$

To make the integral term in the third equation easier to handle, we introduce a new auxiliary variable,

$$y_4(t) = \int_{-\infty}^{t} F(t - s)\, y_3(s)\, ds.$$

Substituting this into the third equation gives,

$$\frac{dy_3}{dt} = \delta y_4 - y_2 y_3.$$

Under suitable regularity conditions on F, it is known that $y_4(t)$ satisfies the following differential equation:

$$\frac{dy_4}{dt} = -d y_4 + d y_3,$$

where d is a constant related to the shape of the kernel F. The delay kernel $F(\cdot)$ is defined in the interval $[0, \infty)$ and is assumed to be nonnegative, bounded, and to satisfy the following conditions:

$$\int_0^{\infty} F(s)\, ds = 1, \quad \int_0^{\infty} sF(s)\, ds < \infty.$$

A common choice for $F(s)$ is the gamma distribution kernel,

$$F(s) = \frac{d^{p+1} s^p}{p!} e^{-ds}, \quad s \geq 0, \quad d > 0,$$

where d is the rate parameter, and p is a nonnegative integer that determines the shape of the kernel. In particular, when $p = 0$, the kernel takes the form $F(s) = de^{-ds}$, which is known as a weak kernel. When $p = 1$, the kernel is called a strong kernel. In this paper, we focus on the weak kernel case. Under the weak kernel assumption, the model can be written as the following system of four differential equations:

$$\begin{aligned} \frac{dy_1}{dt} &= -y_1 + \frac{y_2 y_3}{1 + y_3}, \\ \frac{dy_2}{dt} &= \alpha y_1(t - \tau) - \beta y_2 + \gamma, \\ \frac{dy_3}{dt} &= \delta y_4 - y_2 y_3, \\ \frac{dy_4}{dt} &= -d y_4 + d y_3. \end{aligned} \tag{2.5}$$

Here, we relabel $\tau_1 = \tau$ for simplicity. The system requires initial data defined on the delay interval $[-\tau, 0]$. The initial conditions are specified as

$$y_1(\upsilon) = \phi_1(\upsilon) \geq 0, \quad y_2(\upsilon) = \phi_2(\upsilon) \geq 0, \quad y_3(\upsilon) = \phi_3(\upsilon) \geq 0, \quad y_4(\upsilon) = \phi_4(\upsilon) \geq 0, \tag{2.6}$$

for all $\upsilon \in [-\tau, 0]$, where the initial function $\phi = (\phi_1, \phi_2, \phi_3, \phi_4)^T \in \mathbb{R}^4_+$ is the continuous function on $[-\tau, 0]$.

3. Positivity, boundedness, and equilibria

The right-hand side of system (2.5) is continuous and locally Lipschitz with respect to the state variables. Hence, by the standard existence and uniqueness theory for functional differential equations [23], system (2.5) admits a unique local solution for the initial condition (2.6). We now show that this solution remains nonnegative.

Proposition 3.1. *The solution of system* (2.5) *with initial condition* (2.6) *remains nonnegative for all* $t \geq 0$ *for which the solution exists.*

Proof. Let

$$Y(t) = (y_1(t), y_2(t), y_3(t), y_4(t))^T.$$

Since the initial functions satisfy

$$\phi_i(\theta) \geq 0, \qquad \theta \in [-\tau, 0], \quad i = 1, 2, 3, 4,$$

the solution is nonnegative on the initial interval.

We prove that the positive cone is invariant. Suppose, to the contrary, that one component becomes negative. Then there exists a first time $t_0 > 0$ and an index $i \in \{1, 2, 3, 4\}$ such that

$$y_i(t_0) = 0, \qquad y_j(t) \geq 0 \quad \text{for all } j = 1, 2, 3, 4 \text{ and } t \in [0, t_0],$$

and

$$y_i'(t_0) < 0.$$

We now check the vector field on each boundary face of $\mathbb{R}^4_+$.

If $y_1(t_0) = 0$, then

$$y_1'(t_0) = -y_1(t_0) + \frac{y_2(t_0)y_3(t_0)}{1 + y_3(t_0)} = \frac{y_2(t_0)y_3(t_0)}{1 + y_3(t_0)} \geq 0.$$

If $y_2(t_0) = 0$, then, since $t_0 - \tau \leq t_0$ and the solution is nonnegative up to t_0,

$$y_2'(t_0) = \alpha y_1(t_0 - \tau) - \beta y_2(t_0) + \gamma = \alpha y_1(t_0 - \tau) + \gamma \geq 0.$$

If $y_3(t_0) = 0$, then

$$y_3'(t_0) = \delta y_4(t_0) - y_2(t_0)y_3(t_0) = \delta y_4(t_0) \geq 0.$$

If $y_4(t_0) = 0$, then

$$y_4'(t_0) = -d y_4(t_0) + d y_3(t_0) = d y_3(t_0) \geq 0.$$

Thus, on every boundary face of the nonnegative cone, the corresponding derivative is nonnegative. This contradicts the assumption that some component crosses from nonnegative to negative values at the first exit time. Therefore, no component can become negative, and the solution remains in $\mathbb{R}^4_+$ for all $t \geq 0$ for which it exists. □

Proposition 3.2. *The solutions* $(y_1(t), y_2(t), y_3(t), y_4(t))$ *of system* (2.5) *are bounded for all* $t \geq 0$*, provided the following conditions hold:*

H1: $\beta > 1$ *and* $\alpha < \min\{1, \beta - 1\}$,
H2: $\frac{4d\gamma}{\beta} > (\delta + d)^2$.

Proof. The proof is divided into two parts. First we consider the boundedness of y_1 and y_2, then the boundedness of y_3 and y_4.

Boundedness of y_1 *and* y_2*:*

Let $H(t) := y_1(t) + y_2(t)$. Using the facts that $\frac{y_2 y_3}{1+y_3} \leq y_2$ and $y_1(t-\tau) \leq \sup_{s\in[t-\tau,t]} y_1(s)$, we compute

$$\begin{aligned}\dot{H}(t) &= y_1'(t) + y_2'(t)\\ &\leq (-y_1 + y_2) + \left(\alpha \sup_{s\in[t-\tau,t]} y_1(s) - \beta y_2 + \gamma\right)\\ &= -y_1 - (\beta - 1)y_2 + \gamma + \alpha \sup_{s\in[t-\tau,t]} y_1(s).\end{aligned}$$

Since $y_1, y_2 \geq 0$, we have

$$y_1 + (\beta - 1)y_2 \geq c\,(y_1 + y_2), \qquad c := \min\{1, \beta - 1\}.$$

Moreover, $\sup_{s\in[t-\tau,t]} y_1(s) \leq \sup_{s\in[t-\tau,t]} H(s)$. Hence,

$$\dot{H}(t) \leq -cH(t) + \alpha \sup_{s\in[t-\tau,t]} H(s) + \gamma.$$

This is a Halanay-type differential inequality [24]. Since $\alpha < c$ by H1, the classical Halanay argument implies that

$$H(t) \leq \frac{\gamma}{c - \alpha} + Me^{-\eta(t-t_0)}, \qquad t \geq t_0,$$

for some constants $\eta > 0$ and $M \geq 0$. Thus, $H(t)$ is bounded, and consequently, $y_1(t)$ and $y_2(t)$ are bounded on $[0, \infty)$.

Furthermore, from $y_2'(t) = \alpha y_1(t-\tau) - \beta y_2(t) + \gamma \geq -\beta y_2(t) + \gamma$, we obtain by direct integration $y_2(t) \geq Ce^{-\beta t} + \frac{\gamma}{\beta}$, where C is a constant. Hence, $\liminf_{t\to\infty} y_2(t) \geq \frac{\gamma}{\beta} =: m > 0$.

Boundedness of y_3 *and* y_4*:*

Consider the subsystem

$$\begin{aligned}y_3'(t) &= \delta\, y_4(t) - y_2(t)\, y_3(t),\\ y_4'(t) &= -d\, y_4(t) + d\, y_3(t),\end{aligned}$$

where $\delta, d > 0$. Define the new function

$$V(t) = y_3(t)^2 + y_4(t)^2.$$

Differentiating along solutions yields

$$V'(t) = 2y_3y_3' + 2y_4y_4' = -2y_2y_3^2 - 2dy_4^2 + 2(\delta + d)y_3y_4.$$

Applying Young's inequality (see [25]), for any $\kappa > 0$,

$$2(\delta + d)y_3y_4 \leq \kappa y_3^2 + \frac{(\delta + d)^2}{\kappa} y_4^2.$$

Hence

$$V'(t) \leq (-2y_2 + \kappa)\, y_3^2 + \left(-2d + \frac{(\delta + d)^2}{\kappa}\right) y_4^2.$$

Since $\liminf_{t\to\infty} y_2(t) \geq m$, there exists $T > 0$ such that $y_2(t) \geq m$ for $t \geq T$. Thus, for $t \geq T$,

$$V'(t) \leq (-2m + \kappa)y_3^2 + \left(-2d + \frac{(\delta + d)^2}{\kappa}\right) y_4^2.$$

Assumption $H2$ guarantees that one can choose $\kappa > 0$ so that

$$-2m + \kappa < 0, \qquad -2d + \frac{(\delta + d)^2}{\kappa} < 0.$$

Therefore, we have

$$V'(t) \leq -\bar{c}\, V(t) \qquad (t \geq T),$$

for some constant $\bar{c} = \min\left\{ -(-2m + \kappa),\ -\left(-2d + \frac{(\delta+d)^2}{\kappa}\right)\right\} > 0$. Gronwall's inequality yields (see [25])

$$V(t) \leq V(T)e^{-\bar{c}(t-T)}, \qquad t \geq T.$$

Thus, $V(t)$ is bounded, and consequently, $y_3(t)$ and $y_4(t)$ are bounded. We conclude that all components $(y_1(t), y_2(t), y_3(t), y_4(t))$ of the solution remain bounded for all $t \geq 0$. □

Proposition 3.2 provides a sufficient boundedness criterion for system (2.5) in a tumor-free stability regime. We now determine the equilibria of the system. In the subsequent Hopf bifurcation analysis, we focus on the parameter region where the positive equilibrium exists.

Theorem 3.3. *The system* (2.5) *has two biologically meaningful equilibrium points:*

i. The tumor-free equilibrium point, denoted by $E_0 = \left(0, \frac{\gamma}{\beta}, 0, 0\right)$*, corresponds to the absence of tumor cells, while the other variables take steady-state values.*

ii. The interior equilibrium point, $E^* = (y_1^*, y_2^*, y_3^*, y_4^*)$ *with all* $y_i^* > 0$*, represents a persistent state showing a stable coexistence between tumor cells and immune system components. The equilibrium values are*

$$y_1^* = \frac{\beta\delta - \gamma}{\alpha}, \quad y_2^* = \delta, \quad y_3^* = \frac{\beta\delta - \gamma}{\gamma + \delta(\alpha - \beta)}, \quad y_4^* = y_3^*. \tag{3.1}$$

Proof. To find the equilibrium points, we set the right-hand sides of system (2.5) to zero.

i. First, consider the case $y_3 = 0$. Substituting this into the third equation of system (2.5) gives $y_4 = 0$. From the first equation, we then get $y_2 = \gamma/\beta$, and substituting this into the second equation yields $y_1 = 0$. Therefore, the tumor-free equilibrium is $E_0 = (0, \gamma/\beta, 0, 0)$.

ii. Next, consider the case $y_3 > 0$. Setting the third equation of (2.5) to zero gives $y_2 = \delta$. Substituting this into the first equation gives

$$y_1 = \frac{y_2 y_3}{1 + y_3} = \frac{\delta y_3}{1 + y_3}.$$

Then, substituting $y_2 = \delta$ and this expression for y_1 into the second equation, we obtain

$$0 = \alpha y_1 - \beta\delta + \gamma = \alpha \cdot \frac{\delta y_3}{1 + y_3} - \beta\delta + \gamma.$$

Solving for y_3 gives the expression for y_3^* in (3.1), and from the steady-state condition of the fourth equation, $y_4^* = y_3^*$.

The equilibrium E^* is biologically meaningful provided that $\alpha\delta > \beta\delta - \gamma > 0$.

□

4. Stability and Hopf bifurcation analysis

4.1. Local stability of equilibrium points

We first discuss the local stability of the tumor-free equilibrium $E_0 = \left(0, \frac{\gamma}{\beta}, 0, 0\right)$. The linearization around E_0 can be written as

$$Y'(t) = A_0(E_0)Y(t) + B_0(E_0)Y(t - \tau),$$

where

$$A_0(E_0) = \begin{pmatrix} -1 & 0 & \frac{\gamma}{\beta} & 0 \\ 0 & -\beta & 0 & 0 \\ 0 & 0 & -\frac{\gamma}{\beta} & \delta \\ 0 & 0 & d & -d \end{pmatrix}, \qquad B_0(E_0) = \begin{pmatrix} 0 & 0 & 0 & 0 \\ \alpha & 0 & 0 & 0 \\ 0 & 0 & 0 & 0 \\ 0 & 0 & 0 & 0 \end{pmatrix}.$$

Therefore, the characteristic equation at E_0 is

$$\det\left(\lambda I - A_0(E_0) - B_0(E_0)e^{-\lambda\tau}\right) = 0,$$

which gives

$$(\lambda + 1)(\lambda + \beta)\left[\lambda^2 + \left(d + \frac{\gamma}{\beta}\right)\lambda + d\left(\frac{\gamma}{\beta} - \delta\right)\right] = 0.$$

Since all parameters are positive, it follows from the Routh–Hurwitz criterion that E_0 is locally asymptotically stable if $\frac{\gamma}{\beta} > \delta$, and unstable if $\frac{\gamma}{\beta} < \delta$. The positive equilibrium E^* is biologically meaningful under the condition $\alpha\delta > \beta\delta - \gamma > 0$. In particular, this condition implies $\delta > \gamma/\beta$. Hence, in the parameter region where the positive equilibrium exists, the tumor-free equilibrium is unstable. Therefore, the following stability and Hopf bifurcation analysis focuses on the positive equilibrium E^*.

To study the local stability of the positive equilibrium point E^*, we linearize system (2.5) around E^* and obtain its characteristic equation.

The linearized system gives the following characteristic equation,

$$\det\left(\lambda I - A_0(E^*) - B_0(E^*)e^{-\lambda\tau}\right) = 0, \tag{4.1}$$

where the matrices $A_0(E^*)$ and $B_0(E^*)$ are defined as

$$A_0(E^*) = \begin{pmatrix} -1 & \dfrac{y_3^*}{1+y_3^*} & \dfrac{y_2^*}{(1+y_3^*)^2} & 0 \\ 0 & -\beta & 0 & 0 \\ 0 & -y_3^* & -y_2^* & \delta \\ 0 & 0 & d & -d \end{pmatrix}, \tag{4.2}$$

and

$$B_0(E^*) = \begin{pmatrix} 0 & 0 & 0 & 0 \\ \alpha & 0 & 0 & 0 \\ 0 & 0 & 0 & 0 \\ 0 & 0 & 0 & 0 \end{pmatrix}. \tag{4.3}$$

Substituting these matrices into (4.1), we obtain the characteristic equation at E^* as

$$\lambda^4 + a_1\lambda^3 + a_2\lambda^2 + a_3\lambda + a_4 + (b_1\lambda^2 + b_2\lambda + b_3)e^{-\lambda\tau} = 0, \tag{4.4}$$

where the coefficients are given by

$$\begin{aligned} a_1 &= d + y_2^* + \beta + 1, \\ a_2 &= dy_2^* + \beta y_2^* + \beta d - \delta d + d + y_2^* + \beta, \\ a_3 &= \beta d y_2^* - d\delta\beta + dy_2^* + \beta d + \beta y_2^* - d\delta, \\ a_4 &= y_2^* d\beta - d\delta\beta, \\ b_1 &= \alpha\left(-\frac{y_3^*}{1+y_3^*}\right), \\ b_2 &= \alpha\left(-\frac{y_3^*}{1+y_3^*}\right)\left(y_2^* + d - \frac{y_2^*}{1+y_3^*}\right), \\ b_3 &= \alpha\left(-\frac{y_2^* y_3^* d}{1+y_3^*} + d\delta\frac{y_3^*}{1+y_3^*} + d\frac{y_2^* y_3^*}{(1+y_3^*)^2}\right). \end{aligned}$$

We consider now the stability of E^* for the case $\tau = 0$. In this situation, Eq (4.4) becomes

$$\lambda^4 + a_1\lambda^3 + (a_2 + b_1)\lambda^2 + (a_3 + b_2)\lambda + a_4 + b_3 = 0. \tag{4.5}$$

The following lemma provides sufficient criteria ensuring the local asymptotic stability of E^* when $\tau = 0$.

Lemma 4.1. *If the conditions below are satisfied, then the positive equilibrium E^* is locally asymptotically stable for $\tau = 0$.*

H3: $a_1 > 0, \quad a_3 + b_2 > 0, \quad a_4 + b_3 > 0,$
H4: $a_1(a_2 + b_1)(a_3 + b_2) - (a_3 + b_2)^2 - a_1^2(a_4 + b_3) > 0.$

Proof. For $\tau = 0$, Eq (4.5) becomes a fourth-degree polynomial with real coefficients. By the Routh–Hurwitz criterion, all characteristic roots have negative real parts, and consequently, E^* is locally asymptotically stable, provided that conditions $H3$ and $H4$ are satisfied.

□

4.2. Existence of Hopf bifurcation

Next, we study the characteristic equation (4.4) for $\tau \neq 0$ to identify the conditions under which a Hopf bifurcation may occur. A Hopf bifurcation arises when a pair of complex conjugate roots of the characteristic equation cross the imaginary axis, that is, when purely imaginary roots $\lambda = \pm i\omega$ with $\omega > 0$ exist.

Substituting $\lambda = i\omega$ into (4.4) gives

$$(i\omega)^4 + a_1(i\omega)^3 + a_2(i\omega)^2 + a_3(i\omega) + a_4 + (b_1(i\omega)^2 + b_2(i\omega) + b_3)e^{-i\omega\tau} = 0.$$

Simplifying, we obtain

$$\omega^4 - ia_1\omega^3 - a_2\omega^2 + ia_3\omega + a_4 + (-b_1\omega^2 + ib_2\omega + b_3)(\cos\omega\tau - i\sin\omega\tau) = 0.$$

Separating the real and imaginary parts, we have

$$(-b_1\omega^2 + b_3)\cos\omega\tau + b_2\omega\sin\omega\tau = -\omega^4 + a_2\omega^2 - a_4, \tag{4.6}$$

$$(b_1\omega^2 - b_3)\sin\omega\tau + b_2\omega\cos\omega\tau = a_1\omega^3 - a_3\omega. \tag{4.7}$$

Isolating $\cos(\omega\tau)$ and $\sin(\omega\tau)$ from Eqs (4.6) and (4.7), we get

$$\cos\omega\tau = \frac{-(\omega^4 - a_2\omega^2 + a_4)(-b_1\omega^2 + b_3) - b_2\omega(-a_1\omega^3 + a_3\omega)}{(-b_1\omega^2 + b_3)^2 + b_2^2\omega^2}, \tag{4.8}$$

$$\sin\omega\tau = \frac{(-a_1\omega^3 + a_3\omega)(-b_1\omega^2 + b_3) - b_2\omega(\omega^4 - a_2\omega^2 + a_4)}{(-b_1\omega^2 + b_3)^2 + b_2^2\omega^2}. \tag{4.9}$$

To remove τ and find possible $\omega > 0$ that satisfy these equations, we square (4.6) and (4.7) and add them. This yields

$$\omega^8 + p_1\omega^6 + p_2\omega^4 + p_3\omega^2 + p_4 = 0, \tag{4.10}$$

where

$$\begin{aligned} p_1 &= -2a_2 + a_1^2, \\ p_2 &= a_2^2 + 2a_4 - 2a_1a_3 - b_1^2, \\ p_3 &= 2b_1b_3 - b_2^2 - 2a_2a_4 + a_3^2, \\ p_4 &= a_4^2 - b_3^2. \end{aligned}$$

A positive real root ω_0^2 of (4.10) implies that $\lambda = \pm i\omega_0$ is a pair of purely imaginary roots of the characteristic equation (4.4) for some $\tau = \tau_0$. Hence, a Hopf bifurcation may occur at this critical delay value.

Lemma 4.2. *Equation* (4.10) *has at least one positive real root, say* $\omega_0 > 0$*, if* $p_4 < 0$*.*

Proof. Let $z = \omega^2$. Then (4.10) becomes the quartic polynomial

$$p(z) = z^4 + p_1z^3 + p_2z^2 + p_3z + p_4 = 0. \tag{4.11}$$

The polynomial $p(z)$ is continuous on $\mathbb{R}$, and as $z \to +\infty$, $\lim_{z\to\infty} p(z) = +\infty$. Under assumption $p_4 < 0$, we have $p(0) = p_4 < 0$. By the Intermediate Value Theorem, $p(z)$ must cross the z-axis at least once on the positive real axis. Hence, there exists a real number $z_0 > 0$ such that $p(z_0) = 0$. Therefore, $\omega_0 = \sqrt{z_0} > 0$ is a positive real root of (4.10). This confirms the existence of a critical frequency ω_0 at which purely imaginary roots of the characteristic equation appear. □

Given the critical frequency ω_0, we substitute it into the expressions for $\cos(\omega\tau)$ and $\sin(\omega\tau)$ to find the corresponding delay τ_0. We get

$$\tau_0^{(k)} = \begin{cases} \dfrac{1}{\omega_0}\left(\arccos P + 2k\pi\right), & Q \geq 0, \\ \dfrac{1}{\omega_0}\left(2\pi - \arccos P + 2k\pi\right), & Q < 0, \end{cases} \qquad k = 0, 1, 2, \ldots$$

where $P = \cos(\omega_0\tau_0)$ and $Q = \sin(\omega_0\tau_0)$ are defined in Eqs (4.8) and (4.9).

To verify that a Hopf bifurcation occurs as τ crosses τ_0, we check the transversality condition. The following lemma provides this condition.

Lemma 4.3. *The transversality condition*

$$\mathrm{Re}\left\{\frac{d\lambda}{d\tau}\right\}\Big|_{\tau=\tau_0^{(k)}} > 0$$

holds if the following assumption is satisfied:

H5: $m_1 n_1 + m_2 n_2 > 0$,

where

$$\begin{aligned} m_1 &= -b_2\omega_0^2\cos(\omega_0\tau_0) + (b_3\omega_0 - b_1\omega_0^3)\sin(\omega_0\tau_0), \\ m_2 &= b_2\omega_0^2\sin(\omega_0\tau_0) + (b_3\omega_0 - b_1\omega_0^3)\cos(\omega_0\tau_0), \\ n_1 &= -3a_1\omega_0^2 + a_3 + b_2\cos(\omega_0\tau_0) + 2b_1\omega_0\sin(\omega_0\tau_0) \\ &\quad - \tau_0(-b_1\omega_0^2 + b_3)\cos(\omega_0\tau_0) - \tau_0 b_2\omega_0\sin(\omega_0\tau_0), \\ n_2 &= -4\omega_0^3 + 2a_2\omega_0 + 2b_1\omega_0\cos(\omega_0\tau_0) - b_2\sin(\omega_0\tau_0) \\ &\quad + \tau_0(-b_1\omega_0^2 + b_3)\sin(\omega_0\tau_0) - \tau_0 b_2\omega_0\cos(\omega_0\tau_0). \end{aligned}$$

Proof. Differentiating the characteristic equation (4.4) implicitly with respect to τ and treating λ as a function of τ, we obtain

$$\left(\frac{d\lambda}{d\tau}\right)^{-1} = \frac{4\lambda^3 + 3a_1\lambda^2 + 2a_2\lambda + a_3 + (2b_1\lambda + b_2)e^{-\lambda\tau} - \tau(b_1\lambda^2 + b_2\lambda + b_3)e^{-\lambda\tau}}{\lambda(b_1\lambda^2 + b_2\lambda + b_3)e^{-\lambda\tau}}.$$

Setting $\lambda = i\omega_0$ and $\tau = \tau_0^{(k)}$, we separate the numerator into its real and imaginary parts, giving

$$\mathrm{Re}\left\{\left(\frac{d\lambda}{d\tau}\right)^{-1}\right\} = \frac{m_1 n_1 + m_2 n_2}{m_1^2 + m_2^2}.$$

Hence, the transversality condition holds if and only if $m_1 n_1 + m_2 n_2 > 0$. □

According to the Hopf bifurcation theorem in [23], satisfying the above condition implies that the system undergoes a Hopf bifurcation at the critical delay τ_0 where $k = 0$.

Theorem 4.4. *If assumptions* (*H*3)–(*H*5) *hold, then system* (2.5) *experiences a Hopf bifurcation at* $\tau = \tau_0$. *In this case, the equilibrium point* E^* *is locally asymptotically stable for* $\tau \in [0, \tau_0)$ *and becomes unstable when* $\tau > \tau_0$.

In the next section, we use the normal form and center manifold theories to determine the direction, stability, and period of the periodic solutions that bifurcate from E^* near the critical delay.

5. Direction and stability of Hopf bifurcation

In this section, we analyze the direction, stability, and period of the periodic solutions bifurcating from system (2.5) at the critical delay $\tau = \tau_0$. The analysis follows the normal form and center manifold approach developed by Hassard et al. [26]. This method reduces the dynamics near the positive equilibrium to the center manifold associated with the pair of purely imaginary eigenvalues $\pm i\omega_0$ of the characteristic equation.

We first shift the positive equilibrium point $E^* = (y_1^*, y_2^*, y_3^*, y_4^*)$ to the origin by setting $\bar{y}_i = y_i - y_i^*$, $i = 1, 2, 3, 4$. For simplicity, we continue to denote the translated variables by y_i. The time scale is normalized by setting $t \mapsto t/\tau$, so that the delay becomes one, and the bifurcation parameter is defined by $\rho = \tau - \tau_0$. Thus, for $\tau = \tau_0 + \rho$, the system can be written as a functional differential equation on $C = C([-1, 0], \mathbb{R}^4)$:

$$\dot{Y}(t) = L_\rho(Y_t) + F(\rho, Y_t), \tag{5.1}$$

where $Y(t) = (y_1(t), y_2(t), y_3(t), y_4(t))^T$ and $Y_t(\theta) = Y(t + \theta)$ for $\theta \in [-1, 0]$.

The linear operator L_ρ and nonlinear term F are given by

$$L_\rho(\phi) = (\tau_0 + \rho)\left[A_0\phi(0) + B_0\phi(-1)\right], \quad F(\rho, \phi) = (\tau_0 + \rho)\begin{pmatrix} f_1(\phi) \\ 0 \\ f_3(\phi) \\ 0 \end{pmatrix}, \tag{5.2}$$

where

$$f_1(\phi) = \frac{1}{(1 + y_3^*)^2}\phi_2(0)\phi_3(0) - \frac{y_2^*}{(1 + y_3^*)^3}\phi_3^2(0) - \frac{1}{(1 + y_3^*)^3}\phi_2(0)\phi_3^2(0) + \cdots,$$

and

$$f_3(\phi) = -\phi_2(0)\phi_3(0),$$

with $\phi = (\phi_1, \phi_2, \phi_3, \phi_4) \in C$.

By the Riesz representation theorem, the linear operator L_ρ can be represented by a matrix-valued function $\eta(\theta, \rho)$ on $[-1, 0]$. In particular, we take

$$\eta(\theta, \rho) = (\tau_0 + \rho)\left[A_0\delta(\theta) - B_0\delta(\theta + 1)\right],$$

where $\delta(\cdot)$ denotes the Dirac delta function. The infinitesimal generator $A(\rho)$ is defined by

$$A(\rho)\phi(\theta) = \begin{cases} \dfrac{d\phi(\theta)}{d\theta}, & \theta \in [-1, 0), \\ \displaystyle\int_{-1}^{0} d\eta(s, \rho)\phi(s), & \theta = 0, \end{cases}$$

and the nonlinear operator $R(\rho)$ is

$$R(\rho)\phi(\theta) = \begin{cases} 0, & \theta \in [-1, 0), \\ F(\rho, \phi), & \theta = 0. \end{cases}$$

Hence, Eq (5.1) can be written in the abstract form

$$\dot{Y}_t = A(\rho)Y_t + R(\rho)Y_t. \tag{5.3}$$

Let $A^*(\rho)$ denote the adjoint operator of $A(\rho)$. The bilinear form associated with $A(\rho)$ and $A^*(\rho)$ is defined by

$$\langle \psi, \phi \rangle = \overline{\psi}(0)\phi(0) - \int_{-1}^{0} \int_{0}^{\theta} \overline{\psi}(\xi - \theta)\, d\eta(\theta, \rho)\, \phi(\xi)\, d\xi.$$

Since $\pm i\omega_0\tau_0$ are eigenvalues of $A(0)$ and $A^*(0)$, let $q(\theta)$ and $q^*(s)$ be the corresponding eigenvectors satisfying

$$A(0)q(\theta) = i\omega_0\tau_0 q(\theta), \qquad A^*(0)q^*(s) = -i\omega_0\tau_0 q^*(s).$$

They are written as

$$q(\theta) = (1, q_2, q_3, q_4)^T e^{i\omega_0\tau_0\theta}, \qquad q^*(s) = \overline{D}(1, q_2^*, q_3^*, q_4^*)^T e^{i\omega_0\tau_0 s}.$$

Define

$$c_{12} = \frac{y_3^*}{1 + y_3^*}, \qquad c_{13} = \frac{y_2^*}{(1 + y_3^*)^2}.$$

Then the components of the eigenvector q and the adjoint eigenvector q^* are given by

$$\begin{aligned}
q_2 &= \frac{\alpha e^{-i\omega_0\tau_0}}{i\omega_0 + \beta}, \\
q_3 &= \frac{i\omega_0 + 1 - c_{12}q_2}{c_{13}}, \\
q_4 &= \frac{d}{i\omega_0 + d} q_3, \\
q_2^* &= \frac{-i\omega_0 + 1}{\alpha e^{i\omega_0\tau_0}}, \\
q_3^* &= \frac{c_{12} - (-i\omega_0 + \beta)q_2^*}{y_3^*}, \\
q_4^* &= \frac{\delta}{-i\omega_0 + d} q_3^*.
\end{aligned}$$

The normalization condition

$$\langle q^*, q \rangle = 1, \qquad \langle q^*, \overline{q} \rangle = 0$$

gives

$$\overline{D} = \left(1 + \overline{q}_2^* q_2 + \overline{q}_3^* q_3 + \overline{q}_4^* q_4 + \alpha \overline{q}_2^* \tau_0 e^{-i\omega_0\tau_0}\right)^{-1}.$$

Let Y_t be the solution of (5.1) for $\rho = 0$, and define

$$\begin{aligned}
z(t) &= \langle q^*, Y_t \rangle, \\
W(t, \theta) &= Y_t(\theta) - 2\,\mathrm{Re}\{z(t)q(\theta)\} \\
&= Y_t(\theta) - z(t)q(\theta) - \overline{z}(t)\overline{q}(\theta).
\end{aligned} \tag{5.4}$$

On the center manifold C_0, W can be expanded as

$$W(z, \overline{z}, \theta) = W_{20}(\theta)\frac{z^2}{2} + W_{11}(\theta)z\overline{z} + W_{02}(\theta)\frac{\overline{z}^2}{2} + \cdots. \tag{5.5}$$

Using the duality relation between $A(0)$ and $A^*(0)$, the dynamics of $z(t)$ on the center manifold are obtained as

$$\dot{z} = i\omega_0\tau_0 z + g(z, \bar{z}), \tag{5.6}$$

where

$$g(z, \bar{z}) = g_{20}\frac{z^2}{2} + g_{11}z\bar{z} + g_{02}\frac{\bar{z}^2}{2} + g_{21}\frac{z^2\bar{z}}{2} + \cdots. \tag{5.7}$$

The coefficients g_{20}, g_{11}, g_{02}, and g_{21} are calculated by substituting the center manifold expansion into the nonlinear part of the system. The detailed calculation is given in Appendix A. Using these coefficients, we obtain

$$c_1(0) = \frac{i}{2\omega_0\tau_0}\left(g_{11}g_{20} - 2|g_{11}|^2 - \frac{|g_{02}|^2}{3}\right) + \frac{g_{21}}{2}.$$

Then the quantities determining the bifurcation properties are

$$\mu_2 = -\frac{\mathrm{Re}\{c_1(0)\}}{\mathrm{Re}\{\lambda'(\tau_0)\}}, \tag{5.8}$$

$$\beta_2 = 2\,\mathrm{Re}\{c_1(0)\}, \tag{5.9}$$

$$T_2 = -\frac{\mathrm{Im}\{c_1(0)\} + \mu_2\,\mathrm{Im}\{\lambda'(\tau_0)\}}{\omega_0\tau_0}. \tag{5.10}$$

The sign of μ_2 determines the direction of the Hopf bifurcation. If $\mu_2 > 0$, the bifurcation is supercritical, whereas if $\mu_2 < 0$, it is subcritical. The sign of β_2 determines the stability of the bifurcating periodic solutions: they are stable when $\beta_2 < 0$ and unstable when $\beta_2 > 0$. Finally, T_2 describes the variation of the period of the bifurcating periodic solutions.

6. Numerical simulations

For the numerical simulations, we use the same baseline parameter set as in the previous tumor–immune models of Pang et al. [16] and Wang et al. [22], namely $\alpha = 0.3, \beta = 0.6, \gamma = 3.5$, and $\delta = 10$. For these values, the corresponding tumor-present equilibrium was associated with a dormancy-type regime in the earlier model. We use the same parameter background in order to compare the present distributed-delay formulation with the previous discrete-delay setting. The positive equilibrium of system (2.5) is $E^* = (8.33, 10.0, 5.0, 5.0)$, and the initial condition is chosen close to this equilibrium as $Y(0) = (8, 9, 6, 6)$.

First, when the distributed delay coefficient is $d = 0.5$, the linearization near the equilibrium produces a pair of purely imaginary roots $\lambda = \pm i\omega_0$. The corresponding critical frequency is $\omega_0 = 0.0353$, and the critical delay is $\tau_0 = 31.6504$. At this value, the system undergoes a Hopf bifurcation, and periodic oscillations appear. To study the Hopf bifurcation and determine its direction, simulations were carried out for three different delay values with $\Delta = 2$ so that $\tau = \tau_0 - \Delta$, $\tau = \tau_0$, $\tau = \tau_0 + \Delta$. The time evolution of the variables and the corresponding phase trajectories are shown in Figures 1 and 2.

As τ increases beyond τ_0, both the period and amplitude of oscillations increase. For smaller values of d, the exponential kernel decays more slowly, so past tumor densities remain influential for a longer time. In the simulations, this slower memory decay is associated with oscillations occurring on a longer time scale. From the center manifold and normal form analysis, we obtain

$$c_1(0) = -0.0117 - 5.3144i, \qquad \lambda'(\tau_0) = 3.48 \times 10^{-4} - 6.09 \times 10^{-4}i,$$

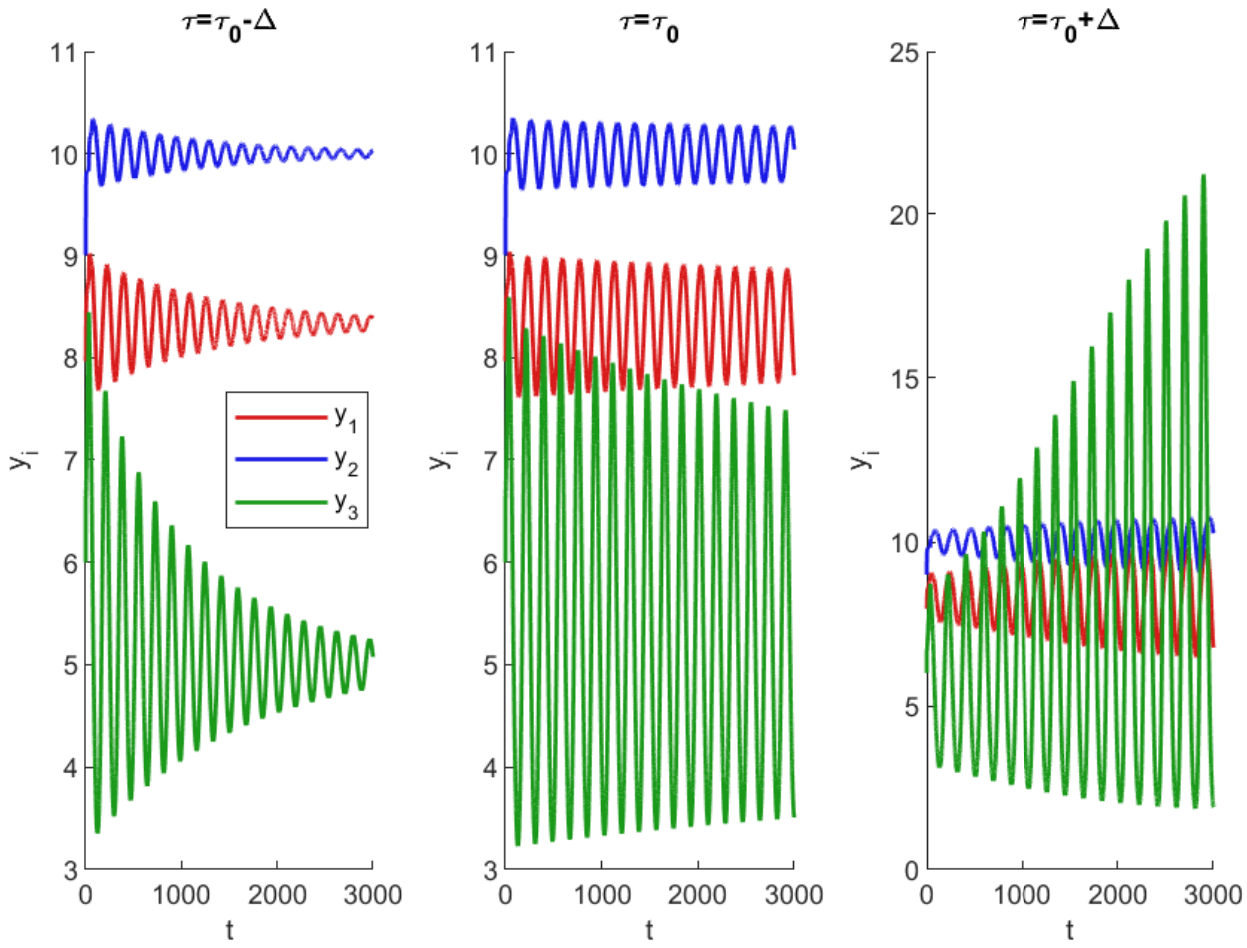

Figure 1. Time evolution of $y_1(t)$, $y_2(t)$, and $y_3(t)$ for $d = 0.5$. The three panels correspond to $\tau = \tau_0 - \Delta$, $\tau = \tau_0$, and $\tau = \tau_0 + \Delta$, where $\tau_0 = 31.6504$ and $\Delta = 2$. The change in the amplitude after crossing τ_0 can be seen from the plots.

which gives

$$\mu_2 = 33.74, \qquad \beta_2 = -0.0235, \qquad T_2 = 4.78.$$

The positive μ_2 and negative β_2 show that the analysis confirms a stable, supercritical Hopf bifurcation. The positive T_2 means that the period increases as τ grows beyond τ_0.

Second, we take the distributed delay coefficient as $d = 4.5$ and perform simulations near the critical delay value with $\Delta = 0.3$. The characteristic equation admits a pair of purely imaginary roots $\lambda = \pm i\omega_0$ with $\omega_0 = 0.2125$, $\tau_0 = 3.1023$, which indicates that a Hopf bifurcation occurs as τ passes through this critical value. For $\tau = \tau_0 - \Delta$, $\tau = \tau_0$, and $\tau = \tau_0 + \Delta$, the corresponding simulation results are shown in Figures 3 and 4.

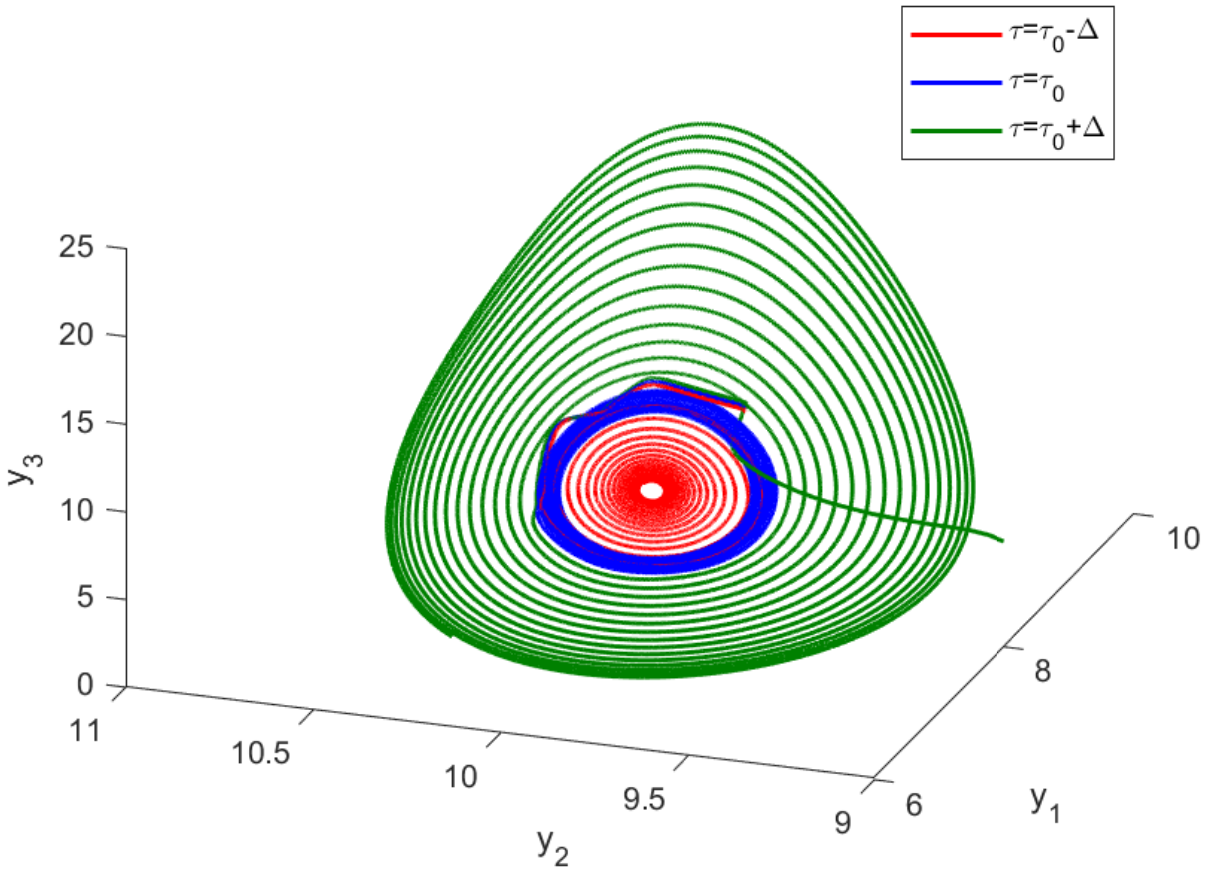

Figure 2. Three-dimensional trajectories in the (y_1, y_2, y_3)-space for $d = 0.5$. The curves are drawn for delay values below, equal to, and above the critical value $\tau_0 = 31.6504$.

The numerical simulations show that when τ exceeds τ_0, the equilibrium loses stability and stable oscillatory behavior appears. In addition, compared with the case of smaller d, the oscillations arise on a shorter time scale.

The center manifold and normal form calculations give

$$c_1(0) = -0.1664 - 0.7496i, \qquad \lambda'(\tau_0) = 1.3946 \times 10^{-2} - 2.0443 \times 10^{-2} i,$$

and hence

$$\mu_2 = 11.9328, \qquad \beta_2 = -0.3328, \qquad T_2 = 1.5068.$$

Since $\mu_2 > 0$ and $\beta_2 < 0$, the Hopf bifurcation is supercritical, and the bifurcating periodic solutions are stable. Moreover, $T_2 > 0$ shows that the period of the bifurcating periodic solutions increases as τ moves beyond the critical value.

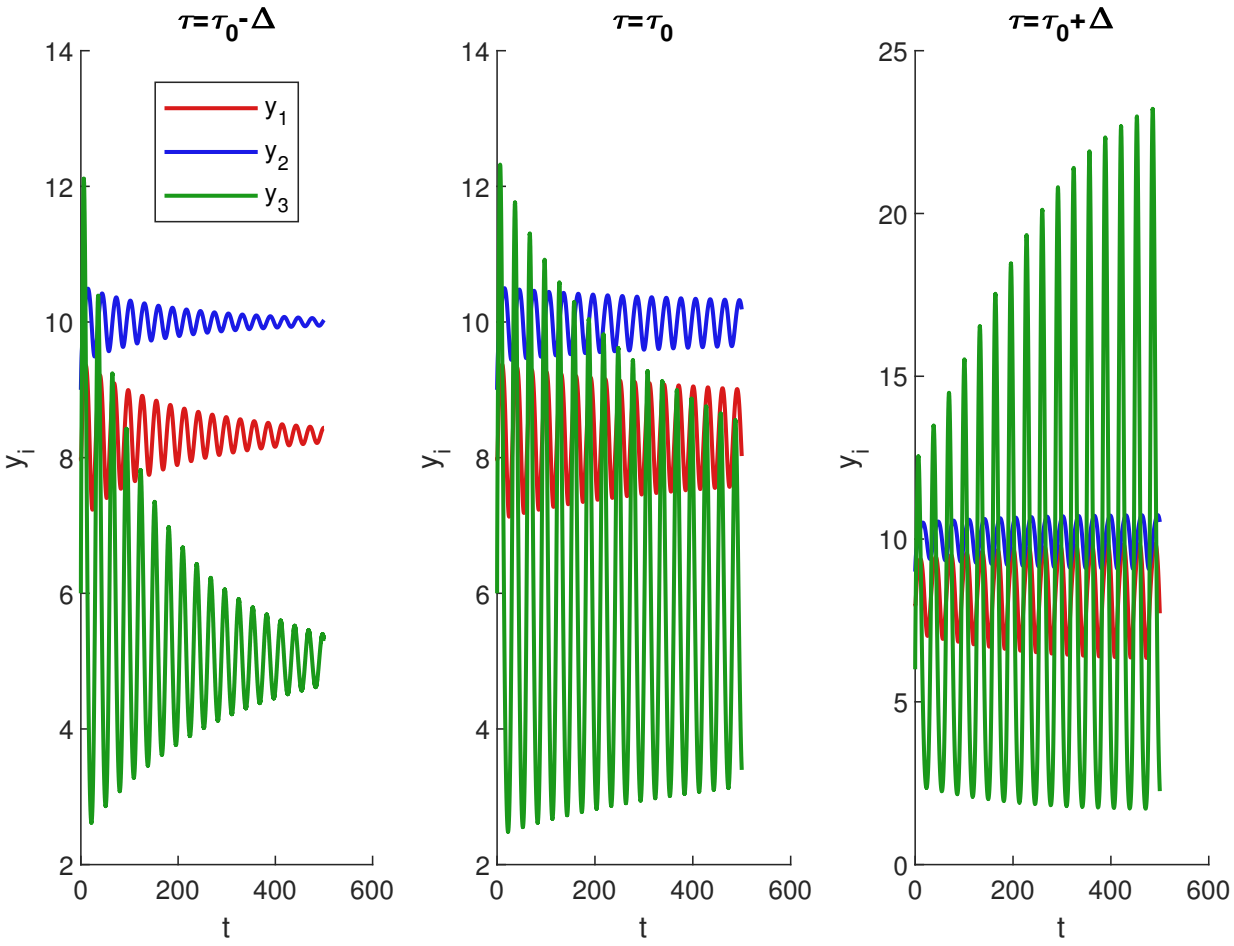

Figure 3. Time evolution of $y_1(t)$, $y_2(t)$, and $y_3(t)$ for $d = 4.5$. The delay is varied around the critical value $\tau_0 = 3.1023$ with $\Delta = 0.3$. Compared with the case $d = 0.5$, the oscillations occur on a shorter time scale.

Finally, we consider the case $d = 8$. In this case, the linearized system has a pair of purely imaginary roots $\lambda = \pm i\omega_0$ with $\omega_0 = 0.2854$, $\tau_0 = 1.7461$, which again indicates the occurrence of Hopf bifurcation.

Simulations are carried out for $\tau \in \{\tau_0 - \Delta, \tau_0, \tau_0 + \Delta\}$ with $\Delta = 0.2$, as shown in Figures 5 and 6. When τ passes through τ_0, the periodic oscillations become more pronounced, and both the amplitude and the period increase.

From the center manifold and normal form calculations, we obtain

$$c_1(0) = -0.005860 - 11.828425\, i, \qquad \lambda'(\tau_0) = 2.679268 \times 10^{-2} - 3.455899 \times 10^{-2}\, i.$$

Therefore,

$$\mu_2 = 0.218733, \qquad \beta_2 = -0.011721, \qquad T_2 = 23.747884.$$

Hence, the Hopf bifurcation is again supercritical, and the bifurcating periodic solutions are stable. The positive value of T_2 shows that the period increases as τ exceeds the critical value.

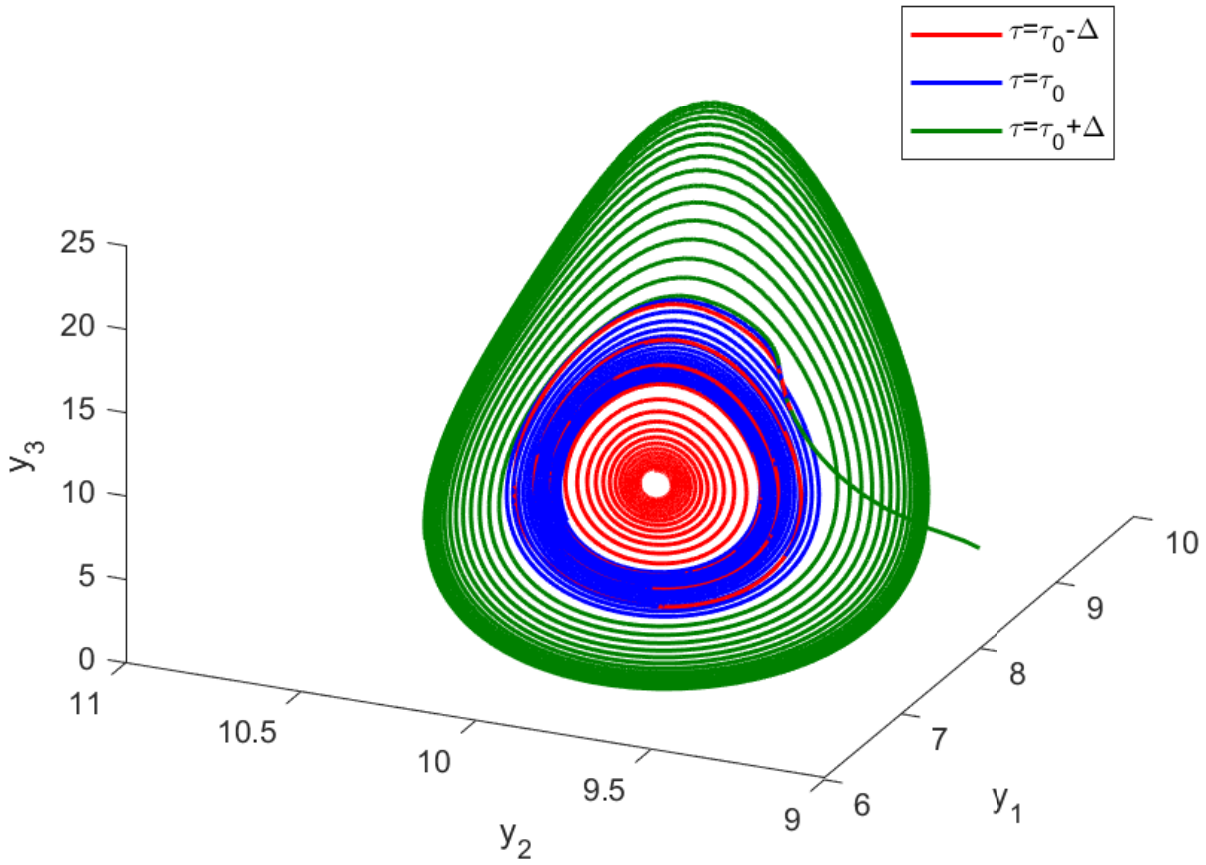

Figure 4. Three-dimensional trajectories in the (y_1, y_2, y_3)-space for $d = 4.5$. The trajectories correspond to $\tau = \tau_0 - \Delta$, $\tau = \tau_0$, and $\tau = \tau_0 + \Delta$.

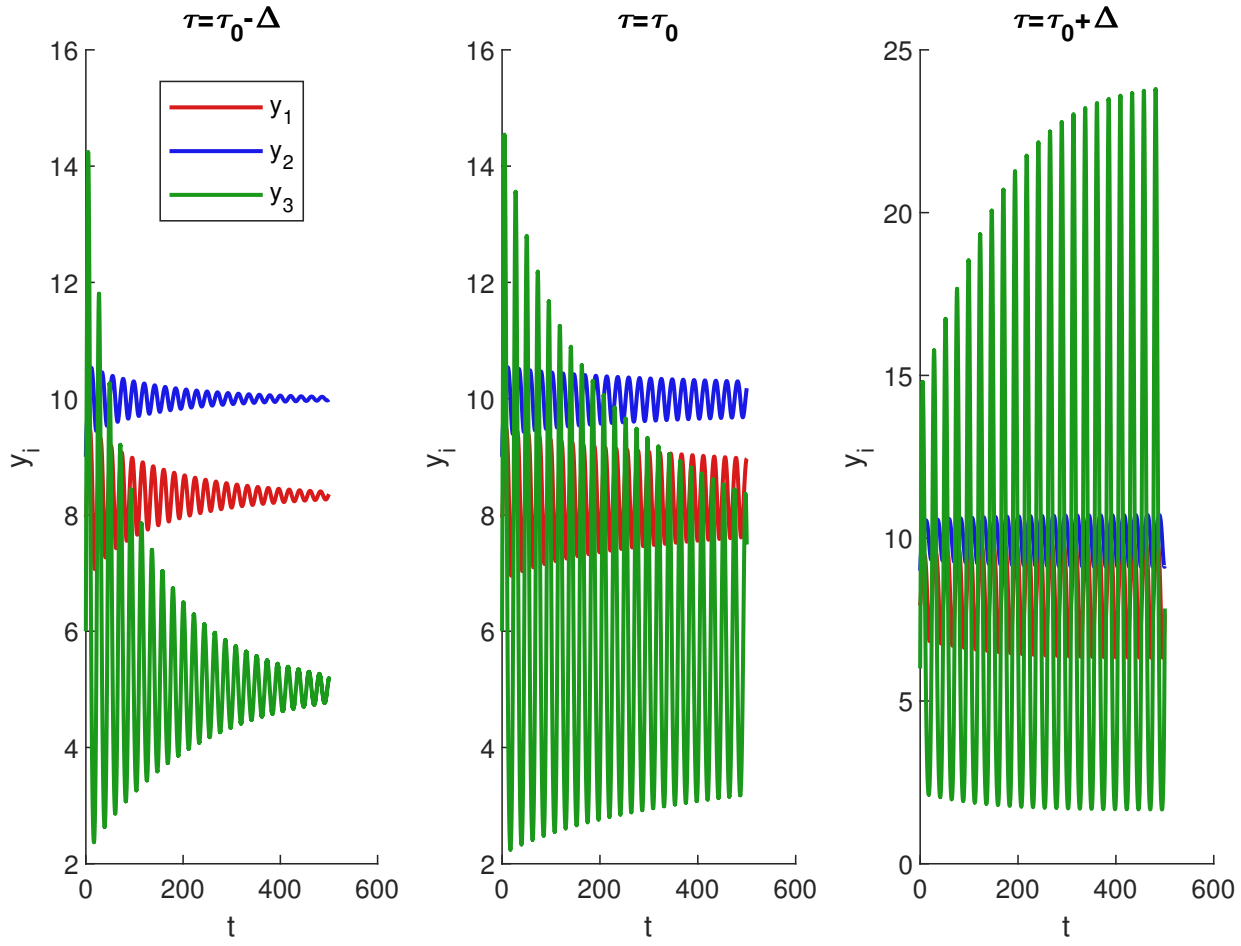

Figure 5. Time evolution of $y_1(t)$, $y_2(t)$, and $y_3(t)$ for $d = 8$. The delay values are chosen near the corresponding critical delay τ_0, showing the solution behavior before and after the bifurcation point.

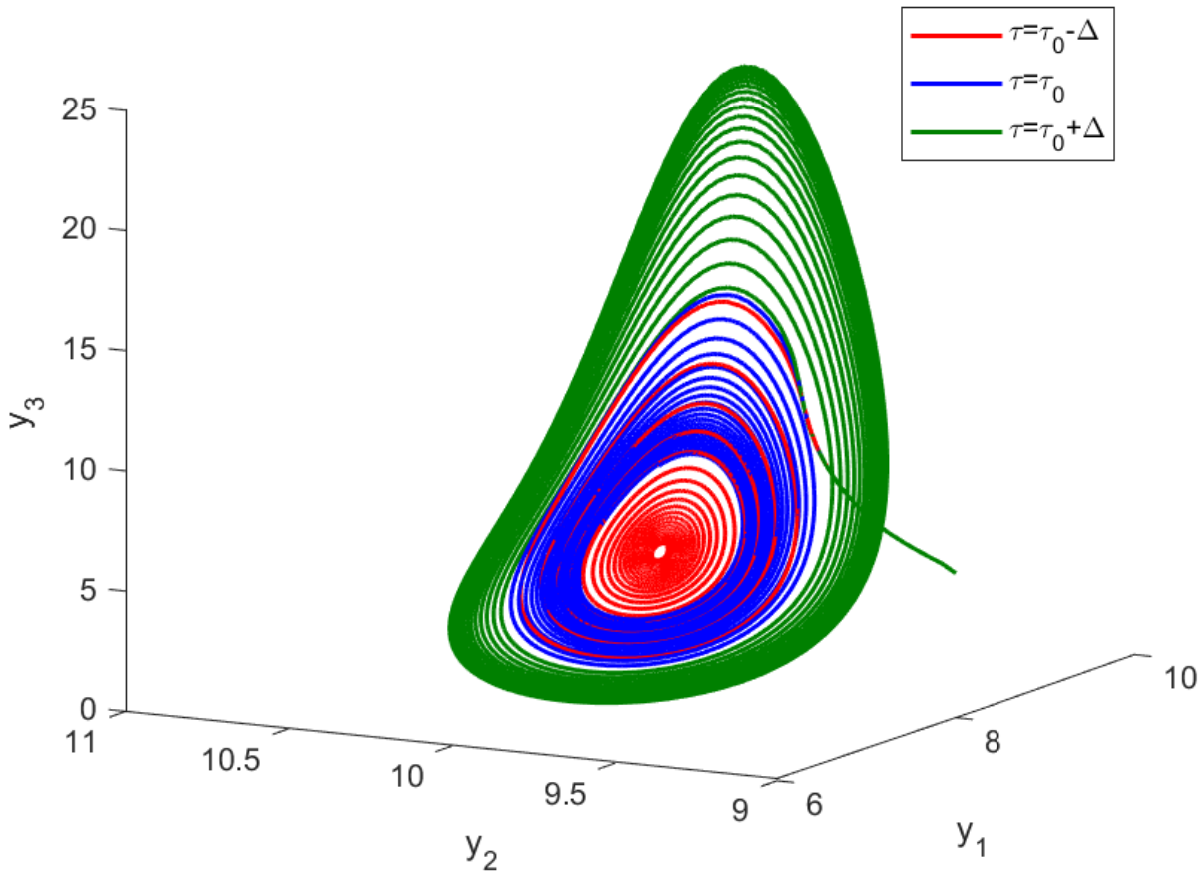

Figure 6. Three-dimensional trajectories in the (y_1, y_2, y_3)-space for $d = 8$. The figure shows how the orbit changes when the delay is varied around the corresponding Hopf value.

The numerical findings agree well with the theoretical Hopf bifurcation analysis. The critical Hopf values and the corresponding normal form quantities for the tested values of d are summarized in Table 1.

Table 1. Critical Hopf values and normal form quantities for different values of the memory-decay parameter d.

d	ω_0	τ_0	μ_2	β_2	T_2
0.5	0.0353	31.6504	33.74	-0.0235	4.78
4.5	0.2125	3.1023	11.9328	-0.3328	1.5068
8	0.2854	1.7461	0.218733	-0.011721	23.747884

As shown in Table 1, increasing d decreases the critical delay τ_0. This suggests that a faster decay of the memory kernel, which gives more weight to recent tumor densities, shifts the Hopf threshold to smaller values of the maturation delay. In all three cases, $\mu_2 > 0$, $\beta_2 < 0$, and $T_2 > 0$, so the Hopf bifurcation is supercritical, the bifurcating periodic solutions are stable, and their period increases after the critical delay is crossed.

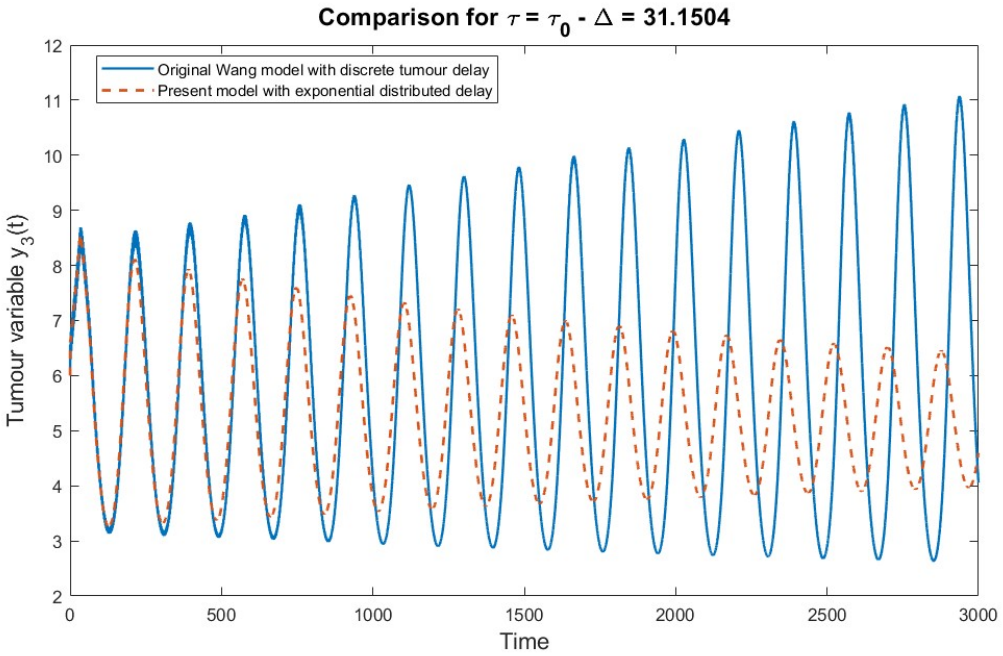

Figure 7. Comparison of the tumor variable $y_3(t)$ in the original model in [22] with a discrete tumor delay and in the present model with an exponential distributed delay for $\tau = \tau_0 - \Delta = 31.1504$. Here, $d = 0.5$, $\tau_2 = 1/d = 2$, and $\Delta = 0.5$.

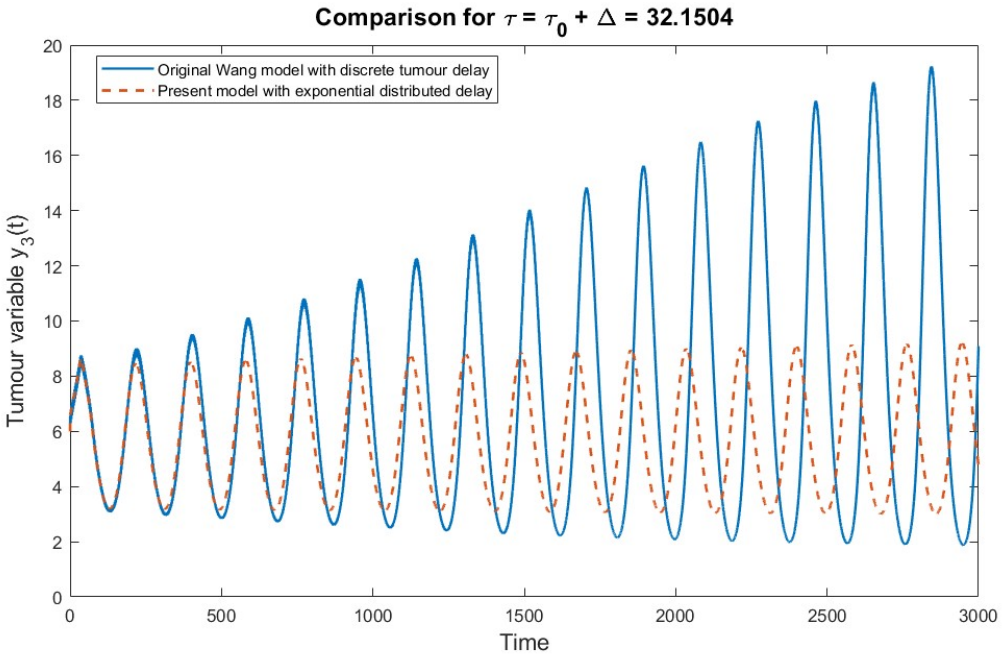

Figure 8. Comparison of the tumor variable $y_3(t)$ in the original model in [22] with a discrete tumor delay and in the present model with an exponential distributed delay for $\tau = \tau_0 + \Delta = 32.1504$. Here, $d = 0.5$, $\tau_2 = 1/d = 2$, and $\Delta = 0.5$.

To compare the present distributed-delay formulation with the original two-discrete-delay model of Wang et al. [22], we performed an additional numerical experiment using the same baseline parameter set. In the original model, the tumor growth term depends on the single delayed value $y_3(t - \tau_2)$. In the present model, this term is replaced by the exponentially distributed memory variable associated with the kernel $F(s) = de^{-ds}$. Since the mean of this kernel is $1/d$, we take $\tau_2 = 1/d$ in the original Wang model for comparison. For $d = 0.5$, this gives $\tau_2 = 2$. We then vary the first delay around the critical value $\tau_0 = 31.6504$ obtained for the present distributed-delay model. The statistics in Table 2 are computed on the post-transient interval $t > 1500$.

Table 2. Post-transient comparison of the tumor variable $y_3(t)$ for the original Wang model and the present distributed-delay model. The statistics are computed for $t > 1500$.

Case	Model	τ	Min y_3	Max y_3	Mean y_3	Amplitude
$\tau_0 - \Delta$	Original Wang model	31.1504	2.6241	11.0780	6.0649	4.2271
$\tau_0 - \Delta$	Present distributed-delay model	31.1504	3.6687	7.0039	5.1258	1.6676
$\tau_0 + \Delta$	Original Wang model	32.1504	1.8760	19.2330	7.7813	8.6783
$\tau_0 + \Delta$	Present distributed-delay model	32.1504	3.0023	9.2185	5.7204	3.1081

Figures 7 and 8 and Table 2 show that both formulations exhibit delay-induced oscillations, but the size of the oscillations differs. In the original Wang model, the tumor variable has a larger post-transient range. For instance, when $\tau = \tau_0 + \Delta$, the amplitude of $y_3(t)$ is approximately 8.6783 in the original model, whereas it is approximately 3.1081 in the present distributed-delay model. Thus, in this parameter setting, replacing the discrete tumor delay by an exponentially distributed memory term reduces the oscillation amplitude. This can be interpreted as a smoothing effect of the distributed delay, since the growth term averages past tumor densities instead of selecting only one past value. The Hopf-type oscillations therefore persist, but their quantitative profile depends on the memory structure.

7. Conclusions

In this paper, we studied a tumor–immune interaction model with one discrete delay and one distributed delay. We derived the characteristic equation at the positive equilibrium and established conditions for local stability. Under suitable parameter conditions, we identified the critical delay at which the equilibrium loses stability and the system undergoes a Hopf bifurcation.

Using center manifold and normal form theory, we computed the bifurcation coefficients and showed that the Hopf bifurcation is supercritical, producing asymptotically stable periodic orbits. The positivity of T_2 further implies that the period of these oscillations increases as the delay passes the critical value. Numerical simulations support the analytical results and illustrate how the kernel parameter affects the amplitude and period of the tumor–immune oscillations.

From a biological perspective, the Hopf bifurcation result shows that the immune-response delay can change the long-term behavior of the tumor–immune system. For delays below the critical value, the positive equilibrium remains stable, corresponding to a steady coexistence of tumor cells and immune components. When the delay exceeds the critical value, this coexistence state loses stability and stable oscillations appear. These oscillations may be interpreted as recurrent phases of tumor growth and delayed immune response.

The distributed delay also affects the form of these oscillations. The parameter d in the exponential kernel $F(s) = de^{-ds}$ controls how fast the memory of past tumor densities decays. Since the mean of this kernel is $1/d$, smaller values of d give more weight to earlier tumor states, whereas larger values of d emphasize more recent states. The numerical results indicate that this memory structure changes the critical delay, amplitude, and period of the tumor–immune oscillations. In particular, increasing d shifts the critical delay τ_0 to smaller values in the tested cases.

Since the present model does not include treatment terms, the results should be interpreted for untreated tumor–immune dynamics. Future work may include chemotherapy or immunotherapy terms, or may consider stronger gamma-type kernels to examine how treatment and more structured memory effects influence the critical delay and the resulting oscillations.

Conflict of interest

The author declares that there is no conflict of interest.

Use of AI tools declaration

The author declares that Artificial Intelligence (AI) tools were used during the preparation of this manuscript. The tool was used only for language editing, improving grammar, and enhancing the clarity and readability of the text. It was not used to generate the mathematical results, numerical simulations, figures, or scientific conclusions.

References

1. M. J. Smyth, D. I. Godfrey, J. A. Trapani, A fresh look at tumor immunosurveillance and immunotherapy, *Nat. Immunol.*, **2** (2001), 293–299. https://doi.org/10.1038/86297
2. C. Parish, Cancer immunotherapy: the past, the present and the future, *Immunol. Cell Biol.*, **81** (2003), 106–113. https://doi.org/10.1046/j.0818-9641.2003.01151.x
3. M. Galach, Dynamics of the tumor–immune system competition—the effect of time delay, *Int. J. Appl. Math. Comput. Sci.*, **13** (2003), 395–406.
4. A. d'Onofrio, A general framework for modeling tumor–immune system competition and immunotherapy: Mathematical analysis and biomedical inferences, *Physica D*, **208** (2005), 220–235. https://doi.org/10.1016/j.physd.2005.06.032
5. M. Sardar, S. Biswas, S. Khajanchi, The impact of distributed time delay in a tumor–immune interaction system, *Chaos, Solitons Fractals*, **142** (2021), 110483. https://doi.org/10.1016/j.chaos.2020.110483
6. S. Banerjee, S. Khajanchi, S. Chaudhury, A mathematical model to elucidate brain tumor abrogation by immunotherapy with T11 target structure, *PLoS One*, **10** (2015), e0123611. https://doi.org/10.1371/journal.pone.0123611
7. L. G. de Pillis, A. Radunskaya, C. L. Wiseman, A validated mathematical model of cell-mediated immune response to tumor growth, *Cancer Res.*, **65** (2005), 7950–7958. https://doi.org/10.1158/0008-5472.can-05-0564

8. L. G. de Pillis, W. Gu, A. E. Radunskaya, Mixed immunotherapy and chemotherapy of tumors: modeling, applications and biological interpretations, *J. Theor. Biol.*, **238** (2006), 841–862. https://doi.org/10.1016/j.jtbi.2005.06.037
9. C. DeLisi, A. Rescigno, Immune surveillance and neoplasia. I. A minimal mathematical model, *Bull. Math. Biol.*, **39** (1977), 201–221. https://doi.org/10.1007/BF02462859
10. A. Rescigno, C. DeLisi, Immune surveillance and neoplasia. II. A two-stage mathematical model, *Bull. Math. Biol.*, **39** (1977), 487–497. https://doi.org/10.1007/BF02462927
11. V. A. Kuznetsov, I. A. Makalkin, M. A. Taylor, A. S. Perelson, Nonlinear dynamics of immunogenic tumors: parameter estimation and global bifurcation analysis, *Bull. Math. Biol.*, **56** (1994), 295–321.
12. L. G. de Pillis, A. E. Radunskaya, A mathematical tumor model with immune resistance and drug therapy: an optimal control approach, *Comput. Math. Methods Med.*, **3** (2001), 79–100. https://doi.org/10.1080/10273660108833067
13. L. G. de Pillis, K. R. Fister, W. Gu, C. Collins, M. Daub, D. Gross, et al., Mathematical model creation for cancer chemo-immunotherapy, *Comput. Math. Methods Med.*, **10** (2009), 165–184. https://doi.org/10.1080/17486700802216301
14. D. Liu, S. Ruan, D. Zhu, Stable periodic oscillations in a two-stage cancer model of tumor and immune system interactions, *Math. Biosci. Eng.*, **9** (2012), 347–368. https://doi.org/10.3934/mbe.2012.9.347
15. L. Pang, Z. Zhao, S. Liu, X. Zhang, Dynamic analysis of an antitumor model and investigation of the therapeutic effects for different treatment regimens, *Comput. Appl. Math.*, **36** (2017), 537–560. https://doi.org/10.1007/s40314-015-0241-4
16. L. Pang, S. Liu, X. Zhang, T. Tian, Mathematical modeling and dynamic analysis of anti-tumor immune response, *J. Appl. Math. Comput.*, **62** (2020), 473–488. https://doi.org/10.1007/s12190-019-01292-9
17. K. Dehingia, H. K. Sarmah, Y. Alharbi, K. Hosseini, Mathematical analysis of a cancer model with time-delay in tumor–immune interaction and stimulation processes, *Adv. Differ. Equations*, **2021** (2021), 473. https://doi.org/10.1186/s13662-021-03621-4
18. P. R. Murugadoss, V. Ambalarajan, V. Sivakumar, P. B. Dhandapani, D. Baleanu, Analysis of dengue transmission dynamic model by stability and Hopf bifurcation with two-time delays, *Front. Biosci. (Landmark Edition)*, **28** (2023), 117. https://doi.org/10.31083/j.fbl2806117
19. M. Sardar, S. Khajanchi, S. Biswas, S. Ghosh, A mathematical model for tumor–immune competitive system with multiple time delays, *Chaos, Solitons Fractals*, **179** (2024), 114397. https://doi.org/10.1016/j.chaos.2023.114397
20. D. Lou, Y. Dai, W. Qin, Bifurcation analysis in a diffusive predator–prey model with distributed memory and gestation delay, *Electron. Res. Arch.*, **33** (2025), 7918–7956. https://doi.org/10.3934/era.2025349
21. J. Li, G. Fan, X. Zhang, H. Zhu, A two-stage model with distributed delay for mosquito population dynamics, *J. Dyn. Differ. Equations*, **38** (2026), 603–626. https://doi.org/10.1007/s10884-025-10431-9

22. J. Wang, H. Shi, L. Xu, L. Zang, Hopf bifurcation and chaos of tumor–Lymphatic model with two time delays, *Chaos, Solitons Fractals*, **157** (2022), 111922. https://doi.org/10.1016/j.chaos.2022.111922
23. J. K. Hale, S. M. V. Lunel, *Introduction to Functional Differential Equations*, Springer-Verlag, 1993. https://doi.org/10.1007/978-1-4612-4342-7
24. A. Halanay, *Differential Equations: Stability, Oscillations, Time Lags*, San Diego, CA, USA: Academic, 1966.
25. W. F. Ames, B. G. Pachpatte, *Inequalities for Differential and Integral Equations*, Elsevier, 1997.
26. B. D. Hassard, N. D. Kazarinoff, Y. H. Wan, *Theory and Applications of Hopf Bifurcation*, Cambridge University Press, 1981.

Appendix: Detailed calculation of the normal form coefficients

In this appendix, we give the algebraic details used in the computation of the normal form coefficients in Section 5.

From (5.4) and (5.5), we write

$$Y_t(\theta) = W(t,\theta) + zq(\theta) + \overline{z}\,\overline{q}(\theta).$$

Hence,

$$Y_t(0) = z\begin{pmatrix}1\\ q_2\\ q_3\\ q_4\end{pmatrix} + \overline{z}\begin{pmatrix}1\\ \overline{q}_2\\ \overline{q}_3\\ \overline{q}_4\end{pmatrix} + W_{20}(0)\frac{z^2}{2} + W_{11}(0)z\overline{z} + W_{02}(0)\frac{\overline{z}^2}{2} + \cdots,$$

$$Y_t(-1) = z\begin{pmatrix}1\\ q_2\\ q_3\\ q_4\end{pmatrix} e^{-i\omega_0\tau_0} + \overline{z}\begin{pmatrix}1\\ \overline{q}_2\\ \overline{q}_3\\ \overline{q}_4\end{pmatrix} e^{i\omega_0\tau_0} + W_{20}(-1)\frac{z^2}{2} + W_{11}(-1)z\overline{z} + W_{02}(-1)\frac{\overline{z}^2}{2} + \cdots.$$

From the definition of g, we have

$$g(z,\overline{z}) = \tau_0\overline{D}(1,\overline{q_2^*},\overline{q_3^*},\overline{q_4^*})\begin{pmatrix}a_{13}y_{2t}(0)y_{3t}(0) + a_{14}y_{3t}^2(0) + \cdots\\ 0\\ -y_{2t}(0)y_{3t}(0)\\ 0\end{pmatrix},$$

where the coefficients in the Taylor expansion of the nonlinear term f_1 at E^* are

$$a_{13} = \frac{1}{(1+y_3^*)^2}, \qquad a_{14} = -\frac{y_2^*}{(1+y_3^*)^3}.$$

Comparing the coefficients of z^2, $\overline{z}^2$, and $z\overline{z}$ gives

$$g_{20} = 2\overline{D}\tau_0\left(a_{13}q_2q_3 + a_{14}q_3^2 - \overline{q_3^*}q_2q_3\right),$$

$$g_{02} = 2\overline{D}\tau_0\left(a_{13}\overline{q}_2\overline{q}_3 + a_{14}\overline{q}_3^2 - \overline{q_3^*}\overline{q}_2\overline{q}_3\right),$$
$$g_{11} = \overline{D}\tau_0\left[a_{13}(q_2\overline{q}_3 + \overline{q}_2 q_3) + 2a_{14}q_3\overline{q}_3 - \overline{q_3^*}(q_2\overline{q}_3 + \overline{q}_2 q_3)\right].$$

To compute g_{21}, we need $W_{20}(\theta)$ and $W_{11}(\theta)$. By using (5.3) and (5.4), W satisfies

$$\dot{W} = \begin{cases} AW - \mathrm{Re}\{\overline{q^*}(0)F_0 q(\theta)\}, & -1 \le \theta < 0, \\ AW - \mathrm{Re}\{\overline{q^*}(0)F_0 q(\theta)\} + F_0, & \theta = 0, \end{cases} = A(0)W + H(z,\overline{z},\theta), \tag{A.1}$$

where

$$H(z,\overline{z},\theta) = H_{20}(\theta)\frac{z^2}{2} + H_{11}(\theta)z\overline{z} + H_{02}(\theta)\frac{\overline{z}^2}{2} + \cdots.$$

Since

$$\dot{W} = W_z\dot{z} + W_{\overline{z}}\dot{\overline{z}},$$

we obtain

$$(A(0) - 2i\omega_0\tau_0)W_{20}(\theta) = -H_{20}(\theta), \tag{A.2}$$
$$A(0)W_{11}(\theta) = -H_{11}(\theta). \tag{A.3}$$

Moreover,

$$H(z,\overline{z},\theta) = -2\,\mathrm{Re}\{g(z,\overline{z})q(\theta)\} = -g(z,\overline{z})q(\theta) - \overline{g}(z,\overline{z})\overline{q}(\theta).$$

Thus,

$$H_{20}(\theta) = -g_{20}q(\theta) - \overline{g}_{20}\overline{q}(\theta),$$
$$H_{11}(\theta) = -g_{11}q(\theta) - \overline{g}_{11}\overline{q}(\theta).$$

Solving (A.2) and (A.3) gives

$$W_{20}(\theta) = \frac{ig_{20}q(0)}{\omega_0\tau_0}e^{i\omega_0\tau_0\theta} + \frac{i\overline{g}_{02}\overline{q}(0)}{3\omega_0\tau_0}e^{-i\omega_0\tau_0\theta} + E_1 e^{2i\omega_0\tau_0\theta}, \tag{A.4}$$
$$W_{11}(\theta) = -\frac{ig_{11}q(0)}{\omega_0\tau_0}e^{i\omega_0\tau_0\theta} + \frac{i\overline{g}_{11}\overline{q}(0)}{\omega_0\tau_0}e^{-i\omega_0\tau_0\theta} + E_2. \tag{A.5}$$

Here $E_1 = (E_1^{(1)}, E_1^{(2)}, E_1^{(3)}, E_1^{(4)})^T$ and $E_2 = (E_2^{(1)}, E_2^{(2)}, E_2^{(3)}, E_2^{(4)})^T$ are constant vectors.

Using the definition of $A(0)$, we have

$$\int_{-1}^{0} d\eta(\theta)W_{20}(\theta) = 2i\omega_0\tau_0 W_{20}(0) - H_{20}(0),$$

and

$$\int_{-1}^{0} d\eta(\theta)W_{11}(\theta) = -H_{11}(0).$$

The values of $H_{20}(0)$ and $H_{11}(0)$ are

$$H_{20}(0) = -g_{20}q(0) - \overline{g}_{20}\overline{q}(0) + 2\tau_0\begin{pmatrix} a_{13}q_2q_3 + a_{14}q_3^2 \\ 0 \\ -q_2q_3 \\ 0 \end{pmatrix},$$

and

$$H_{11}(0) = -g_{11}q(0) - \overline{g}_{11}\overline{q}(0) + 2\tau_0 \begin{pmatrix} a_{13}\,\mathrm{Re}(q_2\overline{q}_3) + a_{14}|q_3|^2 \\ 0 \\ -\,\mathrm{Re}(q_2\overline{q}_3) \\ 0 \end{pmatrix}.$$

The constant vector E_1 is obtained from

$$ME_1 = 2\begin{pmatrix} a_{13}q_2q_3 + a_{14}q_3^2 \\ 0 \\ -q_2q_3 \\ 0 \end{pmatrix},$$

where

$$M = \begin{pmatrix} 2i\omega_0 + 1 & -\dfrac{y_3^*}{1+y_3^*} & -\dfrac{y_2^*}{(1+y_3^*)^2} & 0 \\ -\alpha e^{-2i\omega_0\tau_0} & 2i\omega_0 + \beta & 0 & 0 \\ 0 & y_3^* & 2i\omega_0 + y_2^* & -\delta \\ 0 & 0 & -d & 2i\omega_0 + d \end{pmatrix}.$$

Therefore,

$$E_1 = 2M^{-1}\begin{pmatrix} a_{13}q_2q_3 + a_{14}q_3^2 \\ 0 \\ -q_2q_3 \\ 0 \end{pmatrix}.$$

Similarly, E_2 is found from

$$NE_2 = 2\begin{pmatrix} a_{13}\,\mathrm{Re}(q_2\overline{q}_3) + a_{14}|q_3|^2 \\ 0 \\ -\,\mathrm{Re}(q_2\overline{q}_3) \\ 0 \end{pmatrix},$$

where

$$N = \begin{pmatrix} 1 & -\dfrac{y_3^*}{1+y_3^*} & -\dfrac{y_2^*}{(1+y_3^*)^2} & 0 \\ -\alpha & \beta & 0 & 0 \\ 0 & y_3^* & y_2^* & -\delta \\ 0 & 0 & -d & d \end{pmatrix}.$$

Thus,

$$E_2 = 2N^{-1}\begin{pmatrix} a_{13}\,\mathrm{Re}(q_2\overline{q}_3) + a_{14}|q_3|^2 \\ 0 \\ -\,\mathrm{Re}(q_2\overline{q}_3) \\ 0 \end{pmatrix}.$$

Finally, g_{21} is computed as

$$g_{21} = 2\overline{D}\tau_0\left[a_{13}\left(q_2W_{11}^{(3)}(0) + q_3W_{11}^{(2)}(0) + \frac{1}{2}\overline{q}_2W_{20}^{(3)}(0) + \frac{1}{2}\overline{q}_3W_{20}^{(2)}(0)\right)\right.$$

$$+ a_{14}\left(2q_3 W_{11}^{(3)}(0) + \overline{q}_3 W_{20}^{(3)}(0)\right)$$
$$- \overline{q_3^*}\left(q_2 W_{11}^{(3)}(0) + q_3 W_{11}^{(2)}(0) + \frac{1}{2}\overline{q}_2 W_{20}^{(3)}(0) + \frac{1}{2}\overline{q}_3 W_{20}^{(2)}(0)\right)\Bigg].$$

Substituting g_{20}, g_{11}, g_{02}, and g_{21} into the expression of $c_1(0)$ gives the normal form coefficients used in Section 5.

AIMS Press